


Development of Titanium Surfaces Oxidized by Electrolytic Plasma, for Biomedical Application

Clodomiro Alves-Junior^{a,b*} , Francisca Geidilany S. de O. Frutuoso^b, Jussier de O. Vitoriano^c,
João Paulo V. Santos^d, Michele Edneide da C. Leitão^d, Ricardo D.M. Cavalcante^e

^aUniversidade Federal Rural do Semiárido, Programa de Pós-Graduação em Ciência e Engenharia dos Materiais, 59625-900, Mossoró, RN, Brasil.

^bUniversidade Federal do Rio Grande do Norte, Programa de Pós-Graduação em Ciências da Saúde, 59078-970, Natal, RN, Brasil.

^cUniversidade Federal do Rio Grande do Norte, Programa de Pós-Graduação em Engenharia Mecânica, 59078-970, Natal, RN, Brasil.

^dUniversidade Federal Rural do Semiárido, Departamento de Engenharia Mecânica, 59625-900, Mossoró, RN, Brasil.

^eUniversidade Federal Rural do Semiárido, Departamento de Engenharia Química, 59625-900, Mossoró, RN, Brasil.

Received: January 12, 2023; Revised: March 21, 2023; Accepted: May 09, 2023

Local drug delivery systems used in dental implants need to have uniform pore size distribution, adequate wettability, chemical composition, and biocompatibility. In the present work, titanium was treated by pulsed plasma electrolytic oxidation (PPEO), using 0.025 M sodium dihydrogen phosphate and 0.25 M calcium acetate as electrolytes, aiming at use in drug delivery systems. Pulse with Ton/Toff (width pulse/repetition time) of 50 μ s/100 μ s or 100 μ s/50 μ s, duty cycle 0,33, and 0.67, respectively, were used. After treatment, Ca/P ratio, wettability, crystalline phase, pore size and distribution were determined. The average pore size ranged from 1.5 μ m to 2.3 μ m according to the increase of energy supplied to the system. Pore distributions with lower dispersion were verified for the Ton/Toff condition of 50 μ s /100 μ s, using a current density of 30 mA/dm². On the other hand, the 100 μ s/50 μ s conditions produce larger pores, but with greater dispersion. In general, conditions with lower currents (30 mA/dm² and 38 mA/dm²) and Ton/Toff ratio = 50/100 were the most appropriate for use in drug delivery systems, due to their size and distribution of uniform pores, greater hydrophilicity, and Ca/P ratio close to desirable (1.67) was obtained.

Keywords: PEO, pulsed plasma, titanium, coatings, oxide.

1. Introduction

Due sua non-toxicity, high specific strength, and good biocompatibility titanium is one of the most used metals in biomedical application¹. However, in applications such as dental implants, a surface that induces bone growth is also desirable². This complex osteointegration process involves several biological processes which occur at the tissue-implant interface³. Since titanium is a bioinert material, surface modifications are desirable to overcome this deficiency. One of the strategies used is to coat the implant with hydroxyapatite to improve the osseointegration cellular response, due to the chemical and crystallographic similarity with the inorganic components of dental and bone tissues⁴. Also modifying the microstructure and/or surface roughness, and wettability, contributes to increased cell adhesion^{5,6}. Currently, the development of local drug-delivery systems in order to decrease the risk of peri-implant infections has attracted attention^{3,7,8}. It is important that these systems contain pores (micro or nanotubes) of controlled dimensions, morphology,

crystallinity and distribution^{9,10}. These numerous desirable properties for titanium implant surfaces can be acquired using the plasma electrolytic oxidation (PEO) technique. In this technique, the titanium surface is polarized anodically in an electrochemical cell, to produce a porous surface, primarily containing titanium oxide¹¹. High voltages (250-750 V) between two electrodes result in short-term plasma microdischarges at the electrode/electrolyte interface. The heating and cooling cycles produced during the appearance and extinction of microdischarges, determine the thermodynamic conditions of this interface, decisively influencing the phase evolution, chemical composition, microstructure, and morphology of the coatings^{12,13}. In the pulsed current PEO, it is possible to control the number and duration of that microdischarge by adjusting the pulse parameter (Ton and Toff)¹⁴⁻¹⁶. It is known that duration time of microdischarges (30 - 300 μ s) and the incubation period between an individual discharge and a cascade (100 -1000 μ s) can be controlled by adjusting the Ton and Toff in these time bands¹⁵. Understanding the correlation between surface properties and current pulse parameters, we

*e-mail: clodomiro.jr@ufersa.edu.br

are proposing a pulsed plasma electrolytic oxidation system, using shorter square current pulses (frequency=6.7 kHz), in order to interrupt microdischarges and thus, the main events of the process. To illustrate the importance of this work, we hypothesized an application in dental implants with drug delivery systems.

2. Experimental Procedures

2.1. Sample preparation

Before plasma oxidation, grade 2 titanium discs (3 mm diameter; 2 mm thick) were electrically connected to a conductive wire. The discs were embedded in resin so that only the surface to be oxidized was exposed. Next the samples were metallographically prepared with a final polishing of 0.25 μm silica, then washed with distilled water, cleaned with alcohol and cotton wool and finally dried for further treatment.

2.2. PEO treatment

The PEO treatment was carried out in an equipment (Figure 1) composed of a glass beaker containing 400 ml of electrolyte solution 0.25M of $\text{Ca}(\text{CH}_3\text{CO}_2)_2 \cdot 2\text{H}_2\text{O}$ and 0.025M of $\text{NaH}_2\text{PO}_4 \cdot 2\text{H}_2\text{O}$, with the sample anodically polarized (Figure 1). Opposite to anode a SAE 304 stainless steel square plate was placed (cathode, 50 mm length; 2.0 mm thick).

Square unipolar pulsed current were combined for two different duty cycles (0.33 and 0.67), using current of 30 A/dm², 38 A/dm², and 45 A/dm², resulting at six experimental conditions (Table 1). The duration of all treatments was fixed at 10 minutes. The solution temperature varied between 25 °C and 30 °C, depending on the current density used.

2.3. Samples characterization

Surface micrographs of the coating were obtained using a high resolution scanning electron microscope (SEM) JSM 6010LA, Jeol. For chemical analysis by energy dispersive spectroscopy (EDS), a Dry SD Hyper X-ray detector (EX-94410T1L11) was used, coupled to the SEM. The number, size and distribution of pores were analyzed from electron micrographs using ImageJ software. The wettability test was performed by measuring the static contact angle using the sessile drop method. Images of the accommodation of a drop of 10 μl of distilled water on the treated surfaces were recorded. The crystallographic phases were analyzed with the aid of an X-ray diffractometer, XRD-6000, Shimadzu,

with Cu K α radiation, operating at 30 kV, in the angular range of 20 ° to 80 °, with a scan speed of 2 degrees per minute. and angular pitch of 0.02°. The phases were identified with the help of the High Score Plus program.

3. Results and Discussion

3.1. Microstructural characterization

Changes in morphology and size were dependent on the process condition (Figure 2). In general, samples treated with lowest current values (30T5/10 and 30T10/5), pores are smaller, more homogeneous, and circular. The other samples present, in addition to the pore structure, a continuous film interconnecting the pores, called pancake's structure, which is a consequence of the strong micro-arcs that occur in the localized melting channels, covering pores and sometimes generating small cracks (Figure 2c). Mainly in Figure 2a, 2b and 2d, some pores protrude beyond the surface, suggesting columnar growth of the oxide, giving rise to nano or microtubes.

These porous structures are particularly important for dental implants, especially when considering local drug delivery systems. They must have a high specific surface area, rough and/or porous topography with the appropriate number, size, and distribution of pores that adequately meet the time required for release of specific drugs^{17,18}. Pores with an average size between 0.4 and 3 μm are those that best accommodate the cells and thus have a better biological response^{19,20}. In the present work, the mean diameters and dispersion of pore values were calculated using the imageJ software from the electron micrographs of the samples. It was verified that the values varied proportionally with the electrical current and pulse width. For the lowest values of current and pulse width (30T5/10), the average diameter

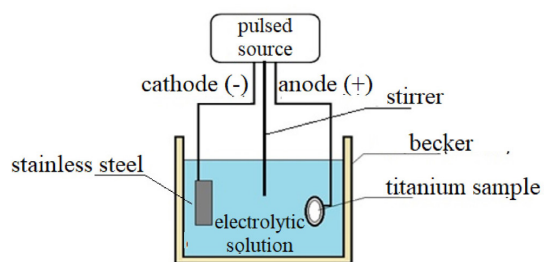


Figure 1. Experimental apparatus to plasma electrolytic oxidation.

Table 1. Experimental conditions for electrolytic plasma oxidation.

Sample	Current Density (A/dm ²)	Ton (μs)	Toff (μs)	Duty cycle (%)
30T5/10	30	50	100	67
38T5/10	38	50	100	67
45T5/10	45	50	100	67
30T10/5	30	100	50	33
38T10/5	38	100	50	33
45T10/5	45	100	50	33

was $0.70 \pm 0.30 \mu\text{m}$, while for the highest values (45T10/5), the average diameter was $1.50 \pm 1.00 \mu\text{m}$. According to the literature, these values are within the desirable range for a good biological response. Regarding the thickness of the coating, an average value of $10 \mu\text{m}$ was obtained from its measurement by profile electron micrograph was found for all experimental conditions, except only for sample 30T5/10, which had a thickness of $25 \mu\text{m}$. This difference can probably be attributed to the detachment of the layer that occurred during the metallographic preparation. A growth rate of $1.0 \mu\text{m min}^{-1}$ is in agreement with the literature for this type of treatment. Considering these pore dimensions, the volume/pore available for drug storage can be calculated by assuming the approximate shape of a hollow cylinder for the pore. These values varied between $3,8 \mu\text{m}^3$ (30T5/10) and $17.7 \mu\text{m}^3$ (45T10/5). Despite the lower volume/pore of samples produced with lower electrical current and pulse

width, these are more interesting for drug delivery systems due to their homogeneity. It is also important to verify that pores with smaller diameters have a greater number of pores per unit area, being $0.14 \text{ pores}/\mu\text{m}^2$ and $0.05 \text{ pores}/\mu\text{m}^2$, for the smallest and largest pore diameters, respectively.

3.2. Chemical analysis

EDS chemical analyzes were carried out throughout the scan region as well as at the points illustrated in Figure 3. Attempts were made to correlate the chemical composition of the film with the distance to the pore, but no consistency was achieved. What can be assumed from this inconsistency is that the process was controlled mainly by surface reaction than by thermal activation. If the oxidation process were thermally activated, it was expected that in the vicinity of the pores there would be a greater formation of TiO_2 , since this region has a higher temperature.

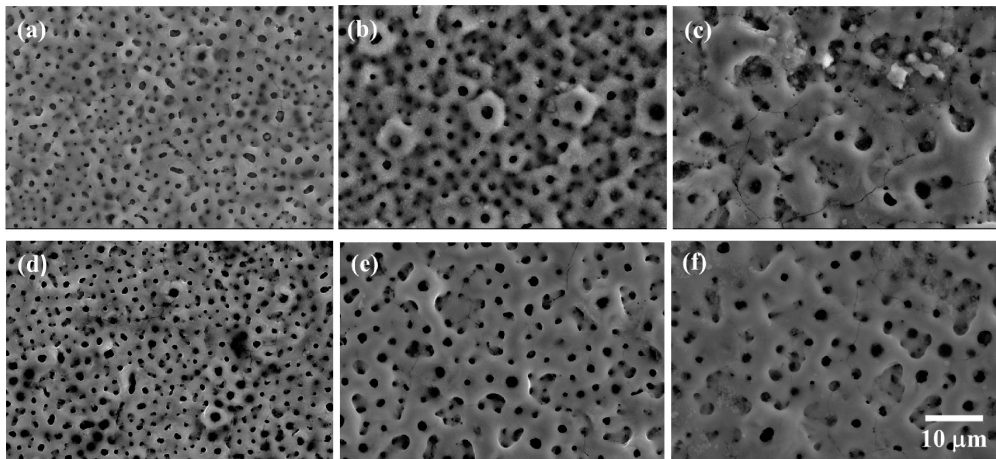


Figure 2. Electron micrograph of samples treated by PEO. (a) 30T5/10, (b) 38T5/10, (c) 45T5/10, (d) 30T10/5, (e) 38T10/5, (f) 45T10/5.

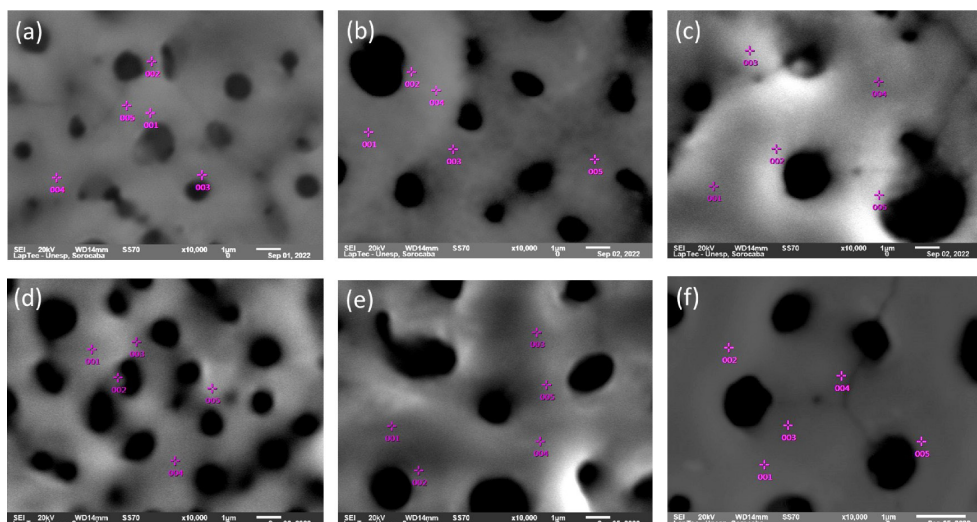
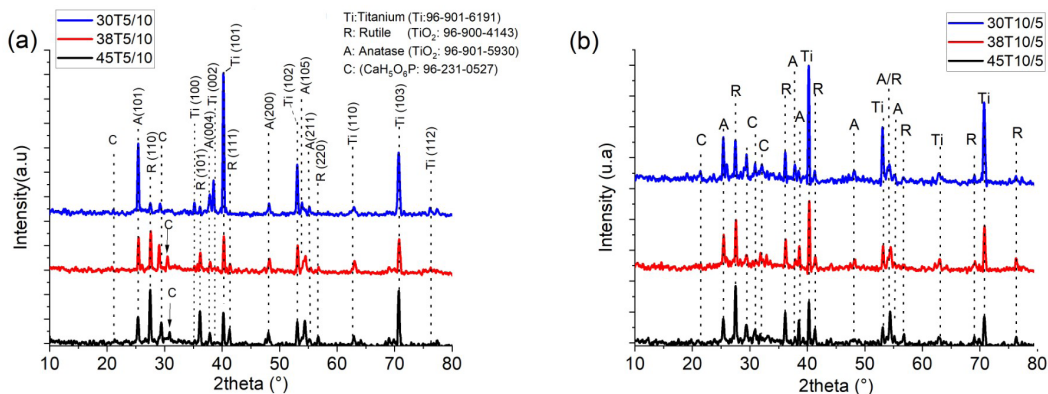


Figure 3. Analyzed scan region, containing the 5 points for punctual analysis.

Table 2. Elemental analysis by EDS of oxidized samples and stoichiometric Ti/O and Ca/P ratios.

Element	Composition (% at)					
	30T5/10	38T5/10	45T5/10	30T10/5	38T10/5	45T10/5
Oxygen	64.43	68.14	65.59	63.26	63.42	58.95
Phosphorus	1.10	4.03	7.11	1.18	0.86	0.84
Calcium	3.50	7.88	6.07	3.94	5.33	6.52
Titanium	30.97	19.95	21.23	31.62	30.39	33.68
Ti/O	0.48	0.29	0.32	0.50	0.48	0.57
Ca/P	3.18	1.96	0.85	3.34	6.19	7.76

**Figure 4.** Diffractogram of samples treated by PEO. (a) duty cycle of 33%; (b) duty cycle of 66%.

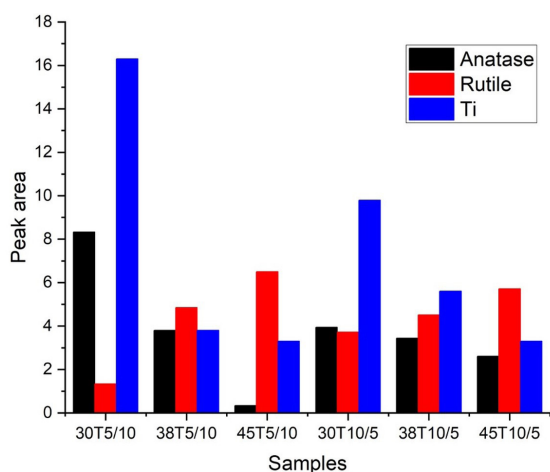
The Ti/O ratio was less than 0.5 (stoichiometric ratio for TiO₂) for the 38T5/10 and 45T5/10 condition (Table 2), indicating that there was no complete formation of TiO₂, unlike the other conditions that presented similar values to 0.5 or greater. In the condition in which there was an excess of oxygen (45T10/5), other oxides such as CaO may have formed.

Regarding the Ca/P ratio, it was observed that the values were generally higher than 1.62 (stoichiometric ratio of hydroxyapatite). However, when these ratios are observed punctually, it is verified that in many cases the stoichiometric ratio was reached. This suggests the existence of dispersed hydroxyapatite particles, and in a heterogeneous way, on the titanium surface.

3.3. Phase identification

Four distinct phases were identified by X-ray diffraction, namely: titanium- α (Ti:96-901-6191), rutile (TiO₂: 96-900-4143), anatase (TiO₂:96-901-5930), and dibasic calcium phosphate (CaH₂O₆P: 96-231-0527).

From the diffractograms (Figure 4), it can be seen that the titanium peaks are more intense for surfaces produced with lower value of electric current. This means that X-ray radiation by oxide films on the titanium surface was lower. That is, although the layer modified by the electrolytic plasma has the same thickness for all conditions, the oxide films have different thicknesses. This means that the oxide films are thinner where the titanium phase peaks were more intense. Another interesting aspect of the diffractogram is that

**Figure 5.** Area of the main peak for anatase, A(101), rutile, R(110), and alpha-Ti, Ti(101), of the x-ray diffractogram.

the peaks referring to the anatase phase vary inversely with the electric current, while for rutile the opposite happens.

After background removal of the X-ray diffraction patterns, the area of the main anatase (25.5°), rutile (27.5°), and titanium (40°) peaks, were calculated (Figure 5).

It is observed that for the same duty cycle, the rutile peak area increases with the current, while the anatase peak area decreases. For $T_{on}=50 \mu s$, the decrease in anatase is more pronounced. It is known from the literature that the anatase

to rutile transformation occurs at temperatures between 450 and 850 °C, respectively²¹.

In the case of PEO, it is estimated that this happens when the electrolyte-film system is around 6 °C²². The temperature and reaction time of the compounds that generate important elements for film formation, such as Ca, P and O, are directly associated with the duration of the pulse repetition. They can occur by the following reactions²³



When titanium is dissolved in the vicinity of the sample (Equation 5), oxygen will be produced and may either evolve as a gas (Equation 6) or dissolves in solution to produce TiO₂ (Equation 7):



Thus, depending on the reaction temperature, anatase or rutile oxides can be produced. Samples oxidized with Ton = 50 μs and Toff = 100 μs tend to produce more anatase due to both the short duration of the microdischarge, 50 μs, and the cooling time of the molten zone by the microdischarge (100 μs).

3.4. Wettability

There is a growing body of literature showing the hydrophilic-hydrophobic conversion of flat titanium dioxide layers induced by irradiating the dry sample with light of a specific wavelength^{24,25}. The wettability of TiO₂ can also vary with topography²⁶, temperature²⁷, and stoichiometric composition²⁸. On TiO₂ surfaces produced by PEO, the size and distribution of pores, in addition to the chemical composition and crystal structure can be controlled. Greater wettability ensures more effective body fluid contact, increasing the initial interaction of proteins with the surface. By controlling the values of polar and non-polar components, one can control the selectivity of fibrinogen and albumin proteins²⁹. The average values of the contact angles observed in our samples (Figure 6) ranged from 55.4° to 106.8°, which means a wide range of character from hydrophilic to hydrophobic. A full discussion of changes in wettability and the influence on the osseointegration and/or drug release lies beyond the scope of this study. Our interest is to advance in this area, carrying out a systematic study of the variation in the wettability of TiO₂ surfaces produced by PEO, when we vary the temperature and surface morphology, irradiating the surface with different UV-Vis wavelengths.

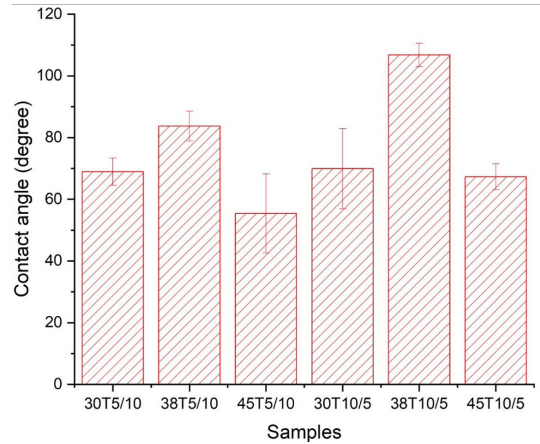


Figure 6. Result of the average values of the contact angles measured and calculated from three samples for each experimental condition.

4. Conclusion

The objective of the present research was to examine the use of PEO with short current pulses (50 and 100 μs) on titanium surfaces, aiming at application in implants, including those with drug delivery systems. This study showed that it was possible to control pore size and distribution, crystalline phase, Ca/P ratio and, still preliminary, wettability. Current data highlights the importance of using smaller pulse widths (50 μs) to achieve greater pore size and uniformity. These results are important because they have pore diameters within the range indicated by the literature for the best cell adhesion response and their values are uniform, providing a homogeneous release of drugs. By reducing the pulse width, it was also possible to obtain a greater amount of anatase, which has better photocatalytic properties. These surfaces, when properly excited by optical radiation, can selectively release drugs. This work contributes to the existing knowledge of new surface modification technologies aimed mainly at biomedical applications.

5. Acknowledgements

The authors are grateful to the National Council for Scientific and Technological Development (CNPq-402536/2021-5 and 304422/2021-5), the National Institute of Surface Engineering (CNPq-465423/2014-0) and the National Council for the Improvement of Higher Education (CAPES) for financial support.

6. References

- Liu X, Chu PK, Ding C. Surface modification of titanium, titanium alloys, and related materials for biomedical applications. *Mater Sci Eng Rep.* 2004;47(3-4):49-121.
- Meng F, Yin Z, Ren X, Geng Z, Su J. Construction of local drug delivery system on titanium-based implants to improve osseointegration. *Pharmaceutics.* 2022;14(5):1069.
- Gulati K, Ivanovski S. Dental implants modified with drug releasing titania nanotubes: therapeutic potential and developmental challenges. *Expert Opin Drug Deliv.* 2017;14(8):1009-24.
- Chamrad J, Marcian P, Cizek J. Beneficial osseointegration effect of hydroxyapatite coating on cranial implant - FEM investigation. *PLoS One.* 2021;16(7):e0254837.

5. Huang HH, Ho CT, Lee TH, Lee TL, Liao KK, Chen FL. Effect of surface roughness of ground titanium on initial cell adhesion. *Biomol Eng.* 2004;21(3-5):93-7.
6. Majhy B, Priyadarshini P, Sen AK. Effect of surface energy and roughness on cell adhesion and growth-facile surface modification for enhanced cell culture. *RSC Advances.* 2021;11(25):15467-76.
7. Pokrowiecki R, Szałaj U, Fudala D, Zaręba T, Wojnarowicz J, Łojkowski W et al. Dental implant healing screws as temporary oral drug delivery systems for decrease of infections in the area of the head and neck. *Int J Nanomedicine.* 2022;17:1679-93.
8. Avila ED, Castro AGB, Tagit O, Krom BP, Löwik D, van Well AA et al. Anti-bacterial efficacy via drug-delivery system from layer-by-layer coating for percutaneous dental implant components. *Appl Surf Sci.* 2019;488:194-204.
9. Lewandowska Ż, Piszczek P, Radtke A, Jędrzejewski T, Kozak W, Sadowska B. The evaluation of the impact of titania nanotube covers morphology and crystal phase on their biological properties. *J Mater Sci Mater Med.* 2015;26(4):1-12.
10. Zhecheva A, Sha W, Malinov S, Long A. Enhancing the microstructure and properties of titanium alloys through nitriding and other surface engineering methods. *Surf Coat Tech.* 2005;200(7):2192-207.
11. Yerokhin AL, Nie X, Leyland A, Matthews A, Doney SJ. Plasma electrolysis for surface engineering. *Surf Coat Tech.* 1999;122(2-3):73-93.
12. Zhang Y, Wu Y, Chen D, Wang R, Li D, Guo C et al. Microstructures and growth mechanisms of plasma electrolytic oxidation coatings on aluminium at different current densities. *Surf Coat Tech.* 2017;321:236-46.
13. Khan RHU, Yerokhin A, Li X, Dong H, Matthews A. Surface characterisation of DC plasma electrolytic oxidation treated 6082 aluminium alloy: effect of current density and electrolyte concentration. *Surf Coat Tech.* 2010;205(6):1679-88.
14. Lima RN, Vitoriano JO, Ferreira M Jr, Alves C Jr. Plasma species and coating compositions in aluminum treated by PEO using shot square pulse. *Mater Res.* 2020;23(3):20190444.
15. Frutuoso FGSO, Vitoriano JO, Alves-Junior C. Controlling plasma electrolytic oxidation of titanium using current pulses compatible with the duration of microdischarges. *Results Mater.* 2022;15:100310.
16. Alves-Junior C, Lima RN, Vitoriano JDO. Pulsed plasma electrolytic oxidation as strategy to produce optical selective surfaces. *IEEE Trans Plasma Sci.* 2022;50(8):2475-81.
17. Roy P, Berger S, Schmuki P. TiO₂ nanotubes: synthesis and applications. *Angew Chem Int Ed.* 2011;50:2904-39.
18. Li L, Xie C, Xiao X. Polydopamine modified TiO₂ nanotube arrays as a local drug delivery system for ibuprofen. *J Drug Deliv Sci Technol.* 2020;56(Pt A):101537.
19. Wang Y, Yu H, Chen C, Zhao Z. Review of the biocompatibility of micro-arc oxidation coated titanium alloys. *Mater Des.* 2015;85:640-52.
20. Martínez Campos E, Santos-Coquillat A, Mingo B, Arrabal R, Mohedano M, Pardo A et al. Albumin loaded PEO coatings on Ti-potential as drug eluting systems. *Surf Coat Tech.* 2015;283:44-51.
21. Hanaor DAH, Sorrell CC. Review of the anatase to rutile phase transformation. *J Mater Sci.* 2011;46:855-74.
22. Casanova L, Vicentini L, Pedferri MP, Ormellese M. Unipolar plasma electrolytic oxidation: waveform optimisation for corrosion resistance of commercially pure titanium. *Mater Corros.* 2021;72(6):1091-104.
23. Liu S, Li B, Liang C, Wang H, Qiao Z. Formation mechanism and adhesive strength of a hydroxyapatite/TiO₂ composite coating on a titanium surface prepared by micro-arc oxidation. *Appl Surf Sci.* 2016;362:109-14.
24. Stevens N, Priest CI, Sedev R, Ralston J. Wettability of photoresponsive titanium dioxide surfaces. *Langmuir.* 2003;19(8):3272-5.
25. Wang R, Hashimoto K, Fujishima A, Chikuni M, Kojima E, Kitamura A et al. Light-induced amphiphilic surfaces. *Nature.* 1997;388:431-2.
26. Shin DH, Shokuhfar T, Choi CK, Lee SH, Friedrich C. Wettability changes of TiO₂ nanotube surfaces. *Nanotechnology.* 2011;22(31):315704.
27. Park JH, Aluru NR. Temperature-dependent wettability on a titanium dioxide surface. *Mol Simul.* 2009;35(1-2):31-7.
28. Lai Y, Huang J, Cui Z, Ge M, Zhang KQ, Chen Z et al. Recent advances in TiO₂-based nanostructured surfaces with controllable wettability and adhesion. *Small.* 2016;12(16):2203-24.
29. Mavropoulos E, Costa AM, Costa LT, Achete CA, Mello A, Granjeiro JM et al. Adsorption and bioactivity studies of albumin onto hydroxyapatite surface. *Colloids Surf B Biointerfaces.* 2011;83(1):1-9.